Wilson, P.A., Lyle, M., and Firth, J.V. (Eds.)
Proceedings of the Ocean Drilling Program, Scientific Results Volume 199

13. Velocity and Density of Paleogene Equatorial Sediments: Variation with Sediment Composition[1]

William H. Busch,[2] Michael D. Vanden Berg,[3] and Pamela E. Masau[2]

ABSTRACT

Sediment density and velocity at the eight sites that comprise the Ocean Drilling Program Leg 199 Pacific Paleogene transect were examined to determine the consistency of the various laboratory and logging measures of density and velocity and the extent to which these parameters vary as a function of sediment composition. Densities were provided in the laboratory by gamma ray attenuation (GRA) in whole-core sections using the GRA sensor and gravimetric and volumetric measurements of discrete samples and from the borehole by GRA using the litho-density tool. Laboratory velocities were obtained for whole-core sections using the *P*-wave logger and for discrete samples using insertion and contact probes. The consistency of bulk densities among the different techniques is very good; however, there is less agreement between the velocities determined by the *P*-wave logger and insertion and contact probes. Variation of density and velocity was compared with the results of the determination of the calcium carbonate content, mineralogy as estimated by light absorption spectroscopy, and bulk sediment geochemistry. Wet bulk density displays a significant dependence on sediment composition, with calcite content being the most important factor influencing density. The amount of opal in the sediment and depth are lesser influences. The sediment velocity does not display a clear relationship with the composition of the sediments.

In situ estimates of density and velocity were determined by comparison of the laboratory and logging values of density and by using published relationships for the derivation of in situ density and velocity

[1] Busch, W.H., Vanden Berg, M.D., and Masau, P.E., 2006. Velocity and density of Paleogene equatorial sediments: variation with sediment composition. *In* Wilson, P.A., Lyle, M., and Firth, J.V. (Eds.), *Proc. ODP, Sci. Results,* 199, 1–31 [Online]. Available from World Wide Web: <http://www-odp.tamu.edu/publications/199_SR/VOLUME/CHAPTERS/226.PDF>. [Cited YYYY-MM-DD]
[2] Department of Geology and Geophysics, University of New Orleans, New Orleans LA 70148, USA. Correspondence author: **wbusch@uno.edu**
[3] Utah Energy Office, Utah Department of Natural Resources, Salt Lake City UT, USA.

Initial receipt: 27 August 2004
Acceptance: 12 October 2005
Web publication: 15 March 2006
Ms 199SR-226

from laboratory measurements. Comparison of laboratory and logging measurements produces equivocal results. A clear trend of increasing elastic rebound in the nannofossil ooze with increasing burial depth is lacking. A larger sample population and greater range of densities is needed to establish a trend in elastic rebound for pelagic clay and radiolarian ooze. The in situ estimates of density and velocity display a distinct character for the different lithologies recovered during Leg 199. Pelagic clay has low bulk density and low velocity. Radiolarian ooze is characterized by uniformly low wet bulk density and unusually high velocity, and nannofossil ooze displays a larger range in bulk density and a more consistent relationship between density and velocity. Because of the variability in velocity, acoustic impedance, calculated from the in situ estimates of the sediment properties, varies primarily as a function of wet bulk density.

INTRODUCTION

During Ocean Drilling Program (ODP) Leg 199, eight sites were sampled in the central tropical Pacific with a focus on Paleogene sediments along a transect on 56- to 57-Ma crust (Fig. F1). The sediments, deposited in the vicinity of the paleoequator, largely consist of a mixture of calcareous and siliceous sediments with lesser amounts of pelagic clay. Sediment density and velocity were routinely measured on core samples at all eight sites and were measured by borehole logging at Sites 1218 and 1219. The objectives of the analysis of the velocity and density measurements at Leg 199 drill sites are to evaluate the consistency of the various core and borehole measurements, to determine the extent to which velocity and density are controlled by sediment composition and burial history, and to estimate the in situ properties of the sediments. Establishing the relationships between density and velocity and estimating the in situ properties of the sediments also serves as a prelude for seismic modeling of the stratigraphy at the Leg 199 drill sites.

F1. Wet bulk densities, p. 13.

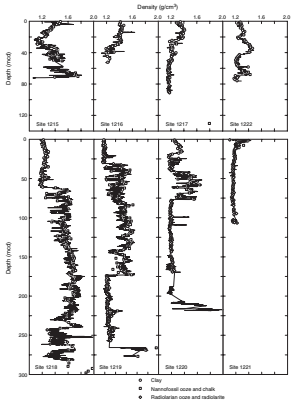

CORE MEASUREMENTS

Density

Two techniques were used during Leg 199 to determine the bulk density of core samples (Lyle, Wilson, Janecek, et al., 2002). Sediment mass and volume measurements were used to determine the wet bulk density of discrete samples of ~10 cm^3 volume. These samples were routinely collected at ~1.5-m intervals. The bulk density of whole-core sections was determined using the gamma ray attenuation (GRA) densiometer on the multisensor track (MST). Measurement of wet bulk density by this device is based on the principle that the attenuation of a collimated beam of gamma rays passing through a known volume is proportional to the material density (Evans, 1965). The measurement width of the GRA sensor is ~5 mm, and the sample spacing was generally set at 4.0 cm for Leg 199 measurements. The narrow width of material sensed and the close sample space allow high-frequency density variation to be recorded; however, it also is accompanied by increased noise in the data. Initial steps in the processing of the GRA records include removing extraneous values and smoothing.

Calibrating the GRA device assumes a two-phase system consisting of minerals and interstitial water (Blum, 1997). An aluminum cylinder represents the mineral phase in the calibration standard. The density of aluminum, 2.70 g/cm^3, is a reasonable approximation for many silicate and carbonate sediment constituents, but it is significantly greater than the density of sediments with appreciable abundances of siliceous components, smectite clays, and zeolites. The average grain density of radiolarian ooze drilled during Leg 199 is ~2.2 g/cm^3. The density of pelagic clays recovered during Leg 199 is more variable, but much of the clayey sediment recovered has average grain densities between 2.4 and 2.6 g/cm^3. As a result of the presence of materials with grain densities lower than that assumed by the calibration method, the GRA density typically was less than the wet bulk density determined for the discrete samples. Incompletely filled core liners can also contribute to low GRA densities. Based on observations of split cores, this factor was judged to be not as significant as grain density differences, particularly for advanced piston corer (APC) cores which comprise the bulk of the Leg 199 cores. Intervals of obviously low GRA densities resulting from incompletely filled cores were removed during data editing. At each of the eight sites drilled during Leg 199, a regression analysis of the wet bulk density and GRA density was performed (Lyle, Wilson, Janecek, et al., 2002). The equations generated by these analyses were applied to the GRA data as a correction in order to make the GRA densities better approximate the wet bulk density of the discrete samples. The agreement between the wet bulk density and the corrected GRA density, which is shown in the depth profiles for the eight sites (Fig. **F1**), is very good. The bulk density in the clay and radiolarian ooze intervals in the profiles typically is very uniform. A higher-frequency variation in bulk density, particularly as recorded by the GRA density, characterizes the nannofossil ooze. The variation of the density in the nannofossil ooze typically follows an alternating lithology resulting from varying abundances of clay and radiolarians.

The crossplot of wet bulk density and corrected GRA density shows a strong correlation between the two density measures (Fig. **F2**). The R^2 value for the regression of GRA density with wet bulk density is 0.91. The crossplot also shows a separation by lithology. The density of the nannofossil ooze and chalk, as a group, is higher than that of the radiolarian ooze and clay. Although the correlation of the two density measures is high, the trend of the regression line shown in Figure **F2** indicates that, despite the correction, the GRA density is less than the wet bulk density of the discrete samples, particularly in the higher-density calcareous sediments.

Despite significant differences in average grain density, variation in wet bulk density primarily is a function of porosity, as displayed by the linear relationship in the crossplot of porosity and wet bulk density (Fig. **F3**). The regression of wet bulk density with porosity has an R^2 value of 0.97. The effect of the differences in grain density is evident in the density-porosity crossplot. At a given porosity value, the density of a radiolarian ooze sample generally is less than that of samples of clay or nannofossil ooze.

Velocity

Three techniques were used to determine the compressional wave velocity of core samples (Lyle, Wilson, Janecek, et al., 2002). The *P*-wave

F2. Wet bulk density vs. GRA density, p. 14.

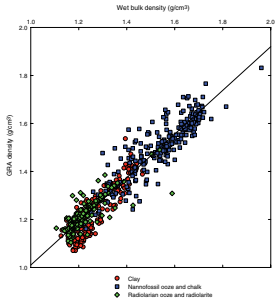

F3. Wet bulk density vs. porosity, p. 15.

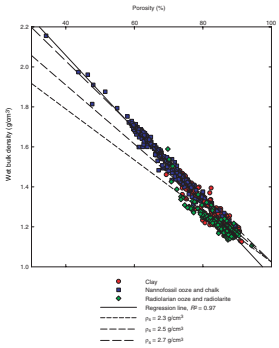

logger (PWL) on the MST was used to measure the horizontal velocity in whole-core samples. The PWL determines the velocity using two transducers aligned perpendicular to the core axis and by measuring the traveltime of a sonic pulse through the sediment and core liner. The velocity of APC cores was determined at a 2-cm spacing with the PWL. The use of the PWL on extended core barrel (XCB) cores was limited by poor acoustic coupling between the sediment and core liner. Velocity measurements were made on split core sections using the insertion and contact probe systems at a spacing of ~1.5 m. The interval for which the velocity was measured coincides with the interval sampled for wet bulk density. The insertion probe system, the successor to the Digital Sonic Velocimeter, was used on soft sediments and consists of two pairs of transducers that are pressed into the sediment, allowing determination of the vertical and horizontal velocity. The depth range over which the insertion probe system was used varied from 0 in radiolarian ooze to depths of 50 meters below seafloor (mbsf) in more clayey sediment. The contact probe system, the successor to the Hamilton Frame, was used on stiff sediments and rocks. The system consists of a fixed and a moveable transducer and can be used to measure the velocity of a split core in its core liner or the velocity of a specimen extracted from the core. Most measurements made with this system during Leg 199 were made with the sediment in the core liner. Velocity measurements of samples outside the core liner were only made for very stiff sediment or rocks that could be cut from the core.

The agreement between the PWL velocity and the velocities determined by the insertion and contact probe techniques, as shown in the velocity profiles for the Leg 199 sites (Fig. **F4**), is not as good as the agreement between the GRA density and the discrete sample wet bulk density. The best correspondence among the different velocities typically occurs in the shallower depths of the holes. At greater depths, the differences between the PWL velocity and contact probe velocity increase for clay and radiolarian ooze. The agreement between the different velocities is better for nannofossil ooze. The crossplot of the insertion and contact probe velocity and the PWL velocity (Fig. **F5**) shows a weak correlation between the discrete sample and MST measurements. The R^2 value for the regression is 0.59. The trend displayed by the data is that PWL velocities are less than the insertion and contact probe velocities, particularly at higher values.

The extent to which velocity variations are controlled by differences in lithology is shown in the crossplot of wet bulk density and velocity (Fig. **F6**). Low wet bulk density characterizes clays (1.1–1.5 g/cm³) and radiolarian oozes (1.1–1.4 g/cm³), and a relationship between velocity and bulk density is lacking. The velocity of the radiolarian oozes (1500–1590 m/s) is slightly higher than that of the clays (1475–1575 m/s). Nannofossil ooze and chalk are characterized by a greater range in wet bulk density and velocity. Most of the nannofossil ooze samples have bulk densities between 1.15 and 1.75 g/cm³ and velocities ranging from 1480 to 1560 m/s. Six chalk samples were collected with densities between 1.8 and 2.2 g/cm³ and velocities from 1600 to 2050 m/s. The pattern of variation in velocity with bulk density in the nannofossil ooze is consistent with that demonstrated for calcareous sediments in previous studies (Mayer et al., 1985; Jarrad et al., 1993). A slight increase in velocity with density characterizes nannofossil oozes with densities less than 1.75 g/cm³ (porosities greater than 55%). The sharp increase in ve-

F4. *P*-wave velocities, p. 16.

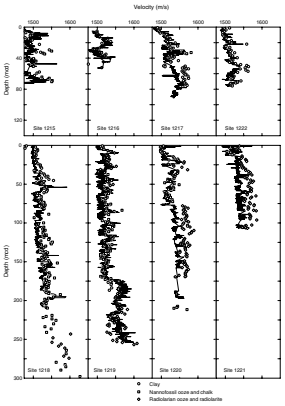

F5. Horizontal *P*-wave velocity vs. PWL velocity, p. 17.

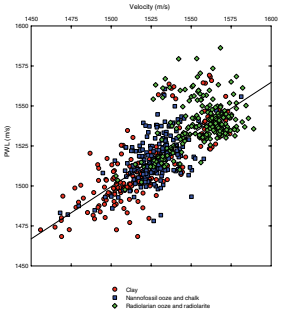

F6. Wet bulk density vs. velocity, p. 18.

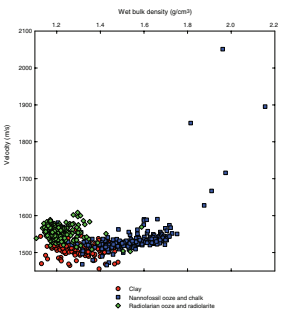

locity in the limited higher-density chalk samples follows the pattern demonstrated for lower-porosity calcareous sediments.

Factors Influencing Density and Velocity

Compositional factors affecting the bulk density and velocity were examined using the mineralogical and bulk chemistry data generated during Leg 199. These data consist of (1) calcium carbonate ($CaCO_3$ in weight percent), determined with a Coulometrics 5011 carbon dioxide coulometer; (2) calcite, opal, illite, and smectite percentages, estimated by light absorption spectroscopy (LAS) (Vanden Berg and Jarrad, 2002); and (3) bulk sediment geochemistry determined by inductively coupled plasma–atomic emission spectroscopy (ICP-AES). Sampling frequency for the composition factors was at least one sample per core for $CaCO_3$ analyses, two samples per section for LAS analyses, and for ICP-AES analyses, one sample per section for Sites 1215 through 1217 and three samples per core for Sites 1218 through 1222. The discrete sample densities and velocities were used in the comparison with mineralogy and bulk chemistry data because the samples for these measurements are either the same (LAS) or immediately adjacent to ($CaCO_3$ and ICP-AES) samples used in the compositional analyses.

The $CaCO_3$ content of the sediments has a significant influence on bulk density and less influence on velocity. The regression of wet bulk density with $CaCO_3$ has an R^2 value of 0.73. The crossplot of wet bulk density and weight percent $CaCO_3$ shows that the relationship between density and $CaCO_3$ depends on lithology (Fig. F7). Density variation in clay is not a function of $CaCO_3$ content. Excluding the clays and considering only the biogenic sediments, the regression of wet bulk density with $CaCO_3$ improves slightly, with $R^2 = 0.79$. The chalk samples with bulk densities higher than 1.8 g/cm³ fall off the trend for density and $CaCO_3$ regression. Loss of intraparticle porosity and reduction of porosity resulting from compaction and cementation may be the cause of the higher density in these materials. Inclusion of depth in the regression of wet bulk density with $CaCO_3$ for all of the samples has a minimal influence, increasing the R^2 value to 0.74. The crossplot of velocity and weight percent $CaCO_3$ (Fig. F8) shows that velocity does not vary as a function of $CaCO^3$ content.

The relationship between wet bulk density and velocity and LAS mineralogy was examined by stepwise multiple regression. Stepwise regression adds one variable at a time to the regression model based on its contribution to explaining the variance in the data. Variables not included in the final model are determined by the procedure to not contribute significantly to explaining the variance. In the regression of density with LAS mineralogy, calcite is the first variable entered into the model, with $R^2 = 0.73$ (Table T1), which matches the results of the regression with weight percent $CaCO_3$. The variables opal, depth, and illite, in that order, were subsequently added in the model, with a final R^2 value of 0.87. In the multiple regression of velocity with depth and the LAS data, depth is the first variable entered, followed by opal and illite (Table T2). The variables in the regression model do a poor job of explaining the variance in velocity. The R^2 value for the model is only 0.25.

Stepwise multiple regression was also used to explore the relationship between wet bulk density and velocity and the bulk sediment

F7. CaO_3 content vs. wet bulk density, p. 19.

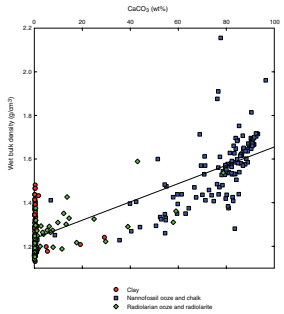

F8. CaO_3 content vs. velocity, p. 20.

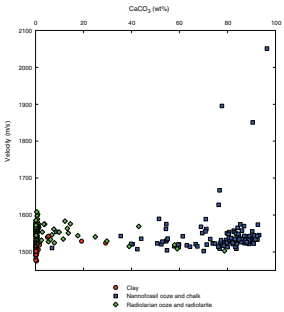

T1. Regression of wet bulk density with LAS data, p. 28.

T2. Regression of velocity with LAS data, p. 29.

geochemistry data. Elements in the bulk sediment data set, in weight percent, include Si, Al, Ti, Fe, Mn, Ca, Mg, P, Sr, and Ba. In the regression of wet bulk density with the geochemistry data, Ca is the first variable entered in the model (R^2 = 0.63) (Table T3). The R^2 value for the overall regression model is 0.87. The association of Ca and calcite is obvious, and its importance in the regression is consistent with the regressions with $CaCO_3$ and LAS mineralogy. Subsequent variables entered in the model largely follow the pattern set in the regression of wet bulk density and LAS data, where the variable order is calcite, opal, depth, and illite. The second variable in the geochemistry model, Ti, occurs in greater abundance in siliceous sediments and clay. Depth, as in the LAS regression, is the third variable entered. The last variables entered in the model, Al and Mg, are those found in greater percentages in clay. The correlation of velocity and the bulk geochemistry data is weak (Table T4); however, the R^2 value of the regression model, 0.47, is higher than that for the model with the LAS data. As in the velocity-LAS regression, depth was determined to be more important than any of the composition-related variables.

T3. Regression of wet bulk density with sediment bulk geochemistry data, p. 30.

T4. Regression of velocity with sediment bulk geochemistry data, p. 31.

BOREHOLE MEASUREMENTS

Two sites were logged during Leg 199, Sites 1218 and 1219. Bulk density measurements were provided by the Hostile Environment Litho-Density Tool (HLDT), and the Dipole Sonic Imager (DSI) was used to measure velocity. The HLDT measures density by irradiating the borehole wall with gamma rays and measuring the flux between the radiation source and the receivers. The source and receivers are pressed against the borehole by an eccentralizing arm. At both Sites 1218 and 1219, the hole diameter over much of the logged intervals is close to or greater than the maximum extent of the eccentralizing arm. Despite the enlarged holes, however, it was determined that there appears to be little deterioration in the data quality of the density logs (Lyle, Wilson, Janecek, et al., 2002). Because of borehole rugosity and the low velocity of the sediments drilled at Sites 1218 and 1219, the sonic logs generated by the DSI are of low quality and were not used.

The character of the density logs matches that displayed by the discrete sample wet bulk density and the GRA density data (Lyle, Wilson, Janecek, et al., 2002). If it is assumed that the logging density accurately represents the in situ sediment bulk density, the amount of elastic rebound experienced by the sediment when it is extracted from the borehole can be estimated by comparing the core and logging data. As a result of elastic rebound and the process of splicing sections from adjacent holes, the length of the composite sections at Sites 1218 and 1219 is longer than the total penetration at each site. In order to compare the core and logging data, the core depths must be compressed and shifted. Because of the closer spacing of the GRA density data, it was used in the correlation with the logging data. The depth profiles of the HLDT logs at Sites 1218 and 1219 and the composite GRA density records shifted to match the HLDT logs are shown in Figure F9. The overall match of the two different density measures at Sites 1218 and 1219 is good; however, the logging density is not consistently larger than GRA density. This pattern is also evident in the crossplot of GRA density and HLDT density (Fig. F10). In the crossplot, GRA density for clay and radiolarian ooze intervals is consistently less than the HLDT density. The values for the nannofossil ooze and chalk are, however, more or less evenly dis-

F9. GRA and HLDT densities, p. 21.

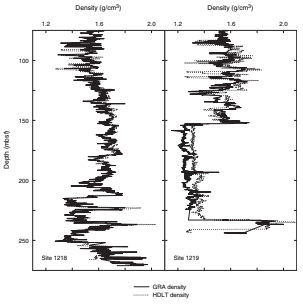

F10. GRA density vs. HLDT density, p. 22.

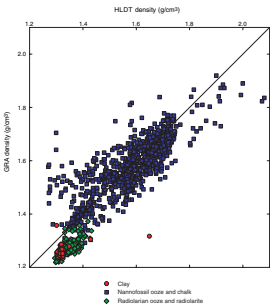

tributed around the one-to-one line for the two density measures. The patterns shown in Figure F10 are not dependent on the selection of the GRA density for the comparison. The same patterns are present when the discrete sample wet bulk density is chosen for comparison with the HLDT density.

ESTIMATION OF IN SITU PROPERTIES

It is commonly recognized that removal of cores from the borehole is accompanied by significant changes in the sediment physical properties. Four factors identified as being responsible for differences between laboratory measurements and in situ properties include (1) temperature change, (2) decrease in hydrostatic pressure, (3) decrease in sediment rigidity, and (4) mechanical rebound resulting in an increase in porosity (Hamilton, 1965, 1976; Mayer et al., 1985; Urmos and Wilkens, 1993).

The rebound experienced by the sediments at Sites 1218 and 1219 was estimated by subtracting the GRA density from the HLDT density. In order to minimize errors associated with the possible mismatch of the two depth profiles, the density difference values were averaged over 5-m windows. The average values for both sites are plotted together in Figure F11 against the effective overburden pressure. Pressure was calculated from the core densities according to the procedure of Busch (1989) and was used instead of depth because of the substantial differences in density among the different lithologies. In addition to the density rebound estimates for Sites 1218 and 1219, curves for predicted density rebound of pelagic clay, radiolarian ooze, and calcareous ooze, derived from the relationships of Hamilton (1976), are shown in Figure F11. The density rebound for the one interval of clay from Site 1219 plots on the predicted pelagic clay rebound line. The density difference for the radiolarian ooze from Sites 1218 and 1219 ranges between ~0.05 and 0.10 g/cm^3. This difference represents a greater expansion than the 0.03–0.04 g/cm^3 predicted from Hamilton (1976) for the range of pressures in which the radiolarian oozes were recovered at Sites 1218 and 1219. The estimated density rebound for the nannofossil ooze and chalk displays no consistent pattern and does not vary as a function of pressure or depth. Over much of the intervals of nannofossil ooze logged at Sites 1218 and 1219, the GRA density from the cores is greater than the HLDT density (Fig. F11). The possible influence of an enlarged borehole on the unexpectedly low HLDT densities was investigated by using the caliper logs to selectively filter the data shown on the crossplot of GRA density and HLDT density for progressively narrower borehole diameters. This filtering did not reveal a dependence of the density patterns on borehole diameter.

Comparison of laboratory and logging density measurements at Sites 1218 and 1219 does not provide a clear path to follow to use the laboratory-determined densities to estimate in situ values. For clays, radiolarian oozes, and radiolarites, the range in values on the density rebound vs. pressure crossplot is insufficient to establish a trend to predict the rebound of samples from the depth that they were extracted. As a conservative estimate, the relationships developed by Hamilton (1976) for estimating porosity rebound were used to derive the in situ density of the clays and siliceous sediments. The calcareous sediments from the logged intervals of Sites 1218 and 1219 pose a different problem in estimating the amount of mechanical rebound. There is a greater range in density rebound values, but they do not follow the prediction from the

F11. Density rebound vs. pressure, p. 23

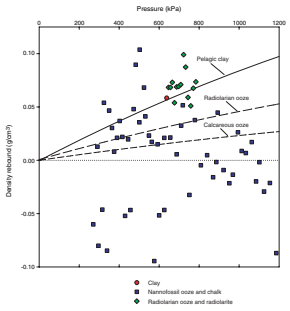

experiments of Hamilton (1976) or any other trend. In an investigation of pelagic carbonates from the Ontong Java Plateau, Urmos and Wilkens (1993) concluded that mechanical rebound did not occur in the carbonate sediments they were studying. Based on this result and the lack of a relationship between density rebound and effective overburden pressure for the nannofossil oozes and chalks at Sites 1218 and 1219, a rebound correction was not applied to estimate the in situ density of the calcareous sediment.

Estimates of in situ wet bulk density and velocity are based on the discrete sample data sets. These data were used because of (1) the unambiguous depth correspondence of the density and velocity samples, (2) the availability of data from XCB cores, and (3) the assumed better quality of the discrete sample data.

The estimated in situ wet bulk density at the Leg 199 sites is shown in Figure **F12** as a composite depth profile combining data from all of the sites. The three principal lithologies, clay, radiolarian ooze, and nannofossil ooze, separate into distinct groupings on the composite depth profile. Pelagic clay, which most commonly occurs in the uppermost 50 m of the sediment columns, displays a moderately wide range in wet bulk density without a distinct downhole trend. The wet bulk density of the radiolarian ooze varies over a narrow range and increases slightly with depth. The nannofossil ooze densities are distinctly higher than those of the radiolarian ooze and more variable without a significant downhole trend.

Estimated porosity, or density, rebound has been used to estimate the effect of mechanical rebound on velocity through using an established velocity-porosity relationship for laboratory measurements (Boyce, 1976; Shipley, 1983; Mayer et al., 1985). In questioning the extent of porosity rebound in pelagic carbonates, Urmos and Wilkens (1993) questioned the appropriateness of using the laboratory measurement extrapolation to estimate the rebound effect on velocity. Because of this doubt and because there is not a well-defined relationship between density and velocity for the Leg 199 sediments (Fig. **F6**), a mechanical rebound correction was not applied to the velocity data.

A correction to account for the effects of the change in temperature and pressure was applied to the laboratory velocity measurements using the approach of Boyce (1976). The pressure in the borehole was assumed to be hydrostatic and was calculated using a seawater density of 1.04 g/cm^3. Results from heat flow measurements at Sites 1218, 1219, and 1220 (Lyle, Wilson, Janecek, et al., 2002) were used to establish an average temperature profile that was applied to all of the Leg 199 sites. The effect of temperature and pressure on the fluid phase of the sediment was estimated using relationships published by Wilson (1960). Following Boyce (1976), it was assumed that temperature and pressure had negligible effect on the velocity of the solid phase of the sediment. Published values of the dry velocity of clay, calcite, and opal were used to calculate the velocity change of the sediment with depth.

The laboratory velocities corrected to estimate the in situ velocity are plotted as a composite depth profile of velocity for the eight Leg 199 sites (Fig. **F13**). The application of the temperature and pressure correction results in a velocity increase of ~1% near the seafloor to ~5% at 300 meters composite depth (mcd). The clays above 50 mcd display the greatest variability in velocity. The radiolarian ooze and radiolarites are characterized by velocities distinctly higher than those of the nannofossil ooze and chalk to a depth of 225 mcd. Below ~225 mcd, velocities of

F12. Composite depths of rebound-corrected wet bulk density, p. 24.

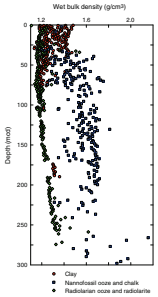

F13. Corrected velocity depth profile, p. 25.

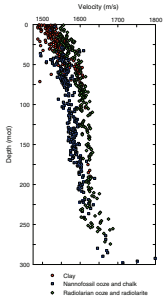

the siliceous and calcareous sediments overlap as a result of the increase in the velocity of the nannofossil ooze and the increased variability of the radiolarian ooze velocity.

The estimated in situ wet bulk density and velocity were used to calculate acoustic impedance. Crossplots of impedance and wet bulk density (Fig. **F14**) and impedance and velocity (Fig. **F15**) indicate that variation in wet bulk density is primarily responsible for differences in impedance. Greater variability in velocity and the lack of consistent velocity trends are largely responsible for the lack of a relationship between velocity and impedance. In both Figure **F14** and Figure **F15,** the radiolarian ooze occupies distinct fields as a result of its overall low density and relatively high velocity.

F14. Corrected wet bulk density and impedance, p. 26.

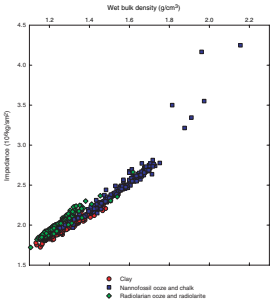

F15. Corrected velocity and impedance, p. 27.

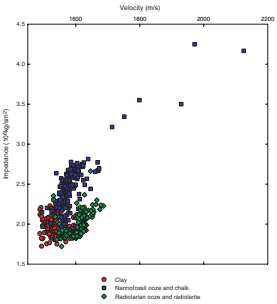

DISCUSSION AND SUMMARY

Review of the velocity and density measurements made during Leg 199 reveals consistent patterns in the variability of the properties and factors that influence them. Velocity tends to display greater variability than density. Overall, the agreement between discrete sample wet bulk density and corrected GRA density is very good. The match between PWL velocity and velocities determined with the insertion and contact probes is weaker. The coring process disrupts the sediment fabric to various degrees, potentially resulting in volumetric changes that affect the bulk density and, consequently, the velocity. The fabric disruption also affects the rigidity of the sediment, which may explain the greater variability displayed by the velocity.

Simple differences in lithology, as determined visually, explain much of the differences in the properties of the sediments. Radiolarian ooze and radiolarite are distinctive in their properties. These sediments display uniformly low bulk densities, even at burial depths greater than 200 m. The siliceous sediments also are characterized by unusually high velocity for their density. There are several possible explanations for this anomaly. One explanation is that the shape of the radiolarians and their interlocking spines creates a stiff sediment framework. Another possibility is that low density results in part from high intraparticle porosity and the relatively large size of radiolarians and low interparticle porosity contribute to greater rigidity of the sediment structure. This latter explanation has been proposed to explain unusually high velocity in foraminifer-rich sediments (Hamilton et al., 1982; Bachman, 1984). As a result of either interlocking spines or low interparticle porosity, increased sediment rigidity produces a higher shear modulus and higher than expected velocities in the siliceous sediments. The pelagic clays, as a group, are characterized by low velocity and low bulk density and lack consistent trends with depth or composition. The properties of the nannofossil ooze are more regular in the relationship between porosity and velocity and the increase in velocity with depth. With increasing burial depth, the transformation to chalk results in a significant velocity increase.

Regression analyses indicate that sediment composition has a significant influence on wet bulk density. Regressions of wet bulk density with weight percent $CaCO_3$, LAS mineralogy, and bulk sediment geochemistry all demonstrate a positive correlation between bulk density and calcium carbonate content. The association between bulk density and weight percent $CaCO_3$ is well established to the extent that GRA density has been used as a proxy for weight percent $CaCO_3$ (Her-

bert and Mayer, 1991; Mayer, 1991; Hagelberg et al., 1995). The high correlation coefficient for the Leg 199 sediments, however, is somewhat deceptive in that the best-fit line is anchored by concentrations of data at approximately zero $CaCO_3$ and between 75 and 95 wt% $CaCO_3$ with a fall off of data from the trend line between these end points (Fig. F7). Results of the regressions of wet bulk density with LAS mineralogy and bulk geochemistry data explain a greater amount of variance in bulk density than the regression with percent $CaCO_3$ alone. Higher R^2 values in these analyses reflect the greater number of variables in the regression models and the larger sample populations. As with the use of the GRA density as a carbonate proxy, Vanden Berg and Jarrad (2004) used a regression of the GRA density with the LAS data to convert the GRA density into a mineralogy proxy.

In contrast to the excellent correlation between the bulk density and the various measures of sediment composition, correlation of the velocity with weight percent $CaCO_3$, LAS mineralogy, and bulk sediment geochemistry is weak to nonexistent. Despite the lack of quantitative relationships between velocity and sediment composition, there are general patterns of differences in velocity among the principal lithologies.

It is difficult to assess the success in estimating in situ values of density and velocity. The agreement between laboratory and logging densities is good, after the laboratory composite sections have been shifted and compressed to match the GRA density with the HLDT density (Fig F9). However, characterizing the elastic rebound by the difference in the logging and laboratory densities produces ambiguous results without a clear relationship between density reduction and overburden pressure or depth (Fig. F11). The lack of clear trends in the mechanical rebound in part results from shallow penetration at Sites 1218 and 1219 and the relatively short overlapping intervals of laboratory and logging densities. The lack of logging velocities limits the evaluation of the in situ velocities estimated from the laboratory data. The extent to which density is primarily responsible for impedance differences may be advantageous in generating synthetic seismograms from density profiles alone. Matching reflectors on the synthetic seismograms with those of the seismic profiles may be the ultimate test of the accuracy of the estimates of in situ density and velocity.

ACKNOWLEDGMENTS

This research used samples and/or data provided by the Ocean Drilling Program (ODP). ODP is sponsored by the U.S. National Science Foundation (NSF) and participating countries under management of Joint Oceanographic Institutions (JOI), Inc. Funding for this research was provided by the U.S. Science Support Program (USSSP). Roy Wilkens and Donna Shillington reviewed the manuscript and provided thoughtful suggestions for its improvement.

REFERENCES

Bachman, R.T., 1984. Intratest porosity in foraminifera. *J. Sediment. Petrol.,* 54:257–262.

Blum, P., 1997. Physical properties handbook: a guide to the shipboard measurement of physical properties of deep-sea cores. *ODP Tech. Note,* 26 [Online]. Available from World Wide Web: <http://www-odp.tamu.edu/publications/tnotes/tn26/INDEX.HTM>. [Cited 2004-08-27]

Boyce, R.E., 1976. Sound velocity-density parameters of sediment and rock from DSDP Drill Sites 315–318 on the Line Island Chain, Manihiki Plateau, and Tuamotu Ridge in the Pacific Ocean. *In* Schlanger, S.O., Jackson, E.D., et al., *Init. Repts. DSDP,* 33: Washington (U.S. Govt. Printing Office), 695–728.

Busch, W.H., 1989. Patterns of sediment compaction at Ocean Drilling Program Sites 645, 646, and 647, Baffin Bay and Labrador Sea. *In* Srivastava, S.P., Arthur, M.A., Clement, B., et al., *Proc. ODP, Sci. Results,* 105: College Station, Texas (Ocean Drilling Program), 781–790.

Evans, H.B., 1965. GRAPE—a device for continuous determination of material density and porosity. *Trans. SPWLA 6th Ann. Logging Symp.:* Dallas, 2:B1–B25.

Hagelberg, T.K., Pisias, N.G., Mayer, L.A., Shackleton, N.J., and Mix, A.C., 1995. Spatial and temporal variability of late Neogene equatorial Pacific carbonate: Leg 138. *In* Pisias, N.G., Mayer, L.A., Janecek, T.R., Palmer-Julson, A., and van Andel, T.H. (Eds.), *Proc. ODP, Sci Results,* 138: College Station, TX (Ocean Drilling Program), 321–336.

Hamilton, E.L., 1965. Sound speed and related properties of sediments from Experimental Mohole (Guadalupe Site). *Geophysics,* 30:257–261.

Hamilton, E.L., 1976. Variations of density and porosity with depth in deep sea sediments. *J. Sediment. Petrol.,* 46:280–300.

Hamilton, E.L., Bachman, R.T., Berger, W.H., Johnson, T.C., and Mayer, L.A., 1982. Acoustic and related properties of calcareous deep-sea sediments. *J. Sediment. Petrol.,* 52:733–753.

Herbert, T.D., and Mayer, L.A., 1991. Long climatic time series from sediment physical property measurements. *J. Sediment. Petrol.,* 61:1089–1108.

Jarrard, R.D., Jackson, P.D., Kasschau, M., and Ladd, J.W., 1993. Velocity and density of carbonate-rich sediments from northeastern Australian margin: integration of core and log data. *In* McKenzie, J.A., Davies, P.J., Palmer-Julson, A., et al., *Proc. ODP, Sci. Results,* 133: College Station, TX (Ocean Drilling Program), 633–647.

Lyle, M., Wilson, P.A., Janecek, T.R., et al., 2002. *Proc. ODP, Init. Repts.,* 199 [CD-ROM]. Available from: Ocean Drilling Program, Texas A&M University, College Station TX 77845-9547, USA.

Mayer, L.A., 1991. Extraction of high-resolution carbonate data for paleoclimate reconstruction. *Nature (London, U.K.),* 352:148–150.

Mayer, L.A., Shipley, T.H., Theyer, F., Wilkens, R.H., and Winterer, E.L., 1985. Seismic modeling and paleoceanography at Deep Sea Drilling Project Site 574. *In* Mayer, L., Theyer, F., Thomas, E., et al., *Init. Repts. DSDP,* 85: Washington (U.S. Govt. Printing Office), 947–970.

Shipley, T.H., 1983. Physical properties, synthetic seismograms, and seismic reflections: correlations at Deep Sea Drilling Project Site 534, Blake-Bahama Basin. *In* Sheridan, R.E., Gradstein, F.M., et al., *Init. Repts. DSDP,* 76: Washington (U.S. Govt. Printing Office), 653–666.

Urmos, J., and Wilkens, R.H., 1993. In situ velocities for pelagic carbonates: new insights from Ocean Drilling Program Leg 130, Ontong Java Plateau. *J. Geophys. Res.,* 98:7903–7920.

Vanden Berg, M.D., and Jarrad, R.D., 2002. Determination of equatorial Pacific mineralogy. *In* Lyle, M., Wilson, P.A., Janecek, T.R., et al., *Proc. ODP, Init. Repts.,* 199

[Online]. Available from World Wide Web: http://www-odp.tamu.edu/publications/199_IR/chap_05/chap_05.htm. [Cited 2004-08-27]

Vanden Berg, M.D., and Jarrad, R D., 2004. Cenozoic mass accumulation rates in the equatorial Pacific based on high-resolution mineralogy of Ocean Drilling Program Leg 199. *Paleoceanography,* 19:PA2021.

Wilson, W.D., 1960. Speed of sound in seawater as a function of temperature, pressure and salinity. *J. Acoust. Soc. Am.,* 32:641–644.

Figure F1. Wet bulk density of moisture content and density samples and GRA density. Depth scale is developed by splicing intervals from adjacent holes at a site to produce a composite section.

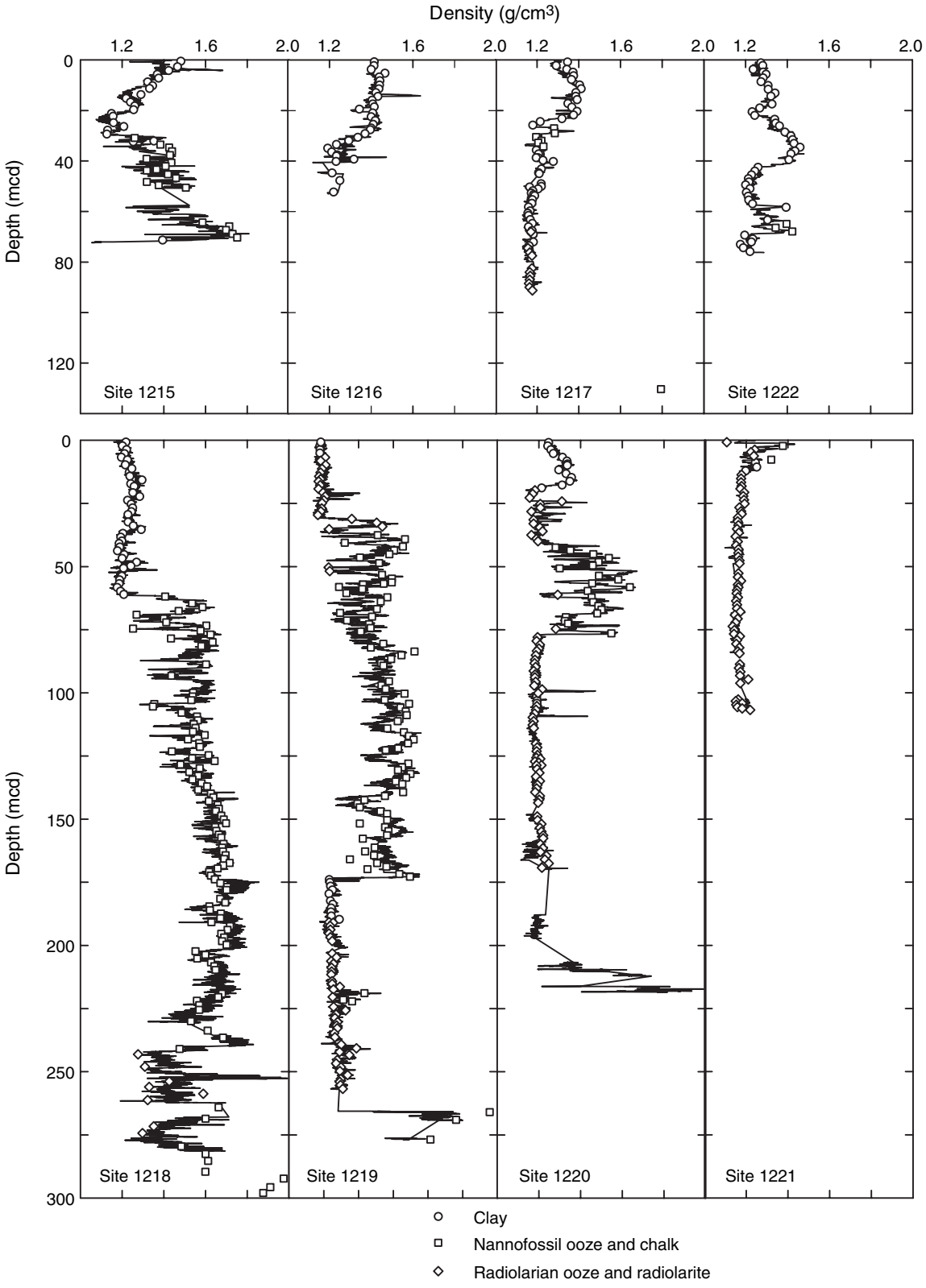

Figure F2. Comparison of wet bulk density of discrete core samples and corrected gamma ray attenuation (GRA) density at the equivalent depth. $R^2 = 0.91$. GRA densities were corrected by applying the results of regression analyses of wet bulk density and GRA density performed for each of the eight sites drilled during Leg 199 (Lyle, Wilson, Janecek, et al., 2002).

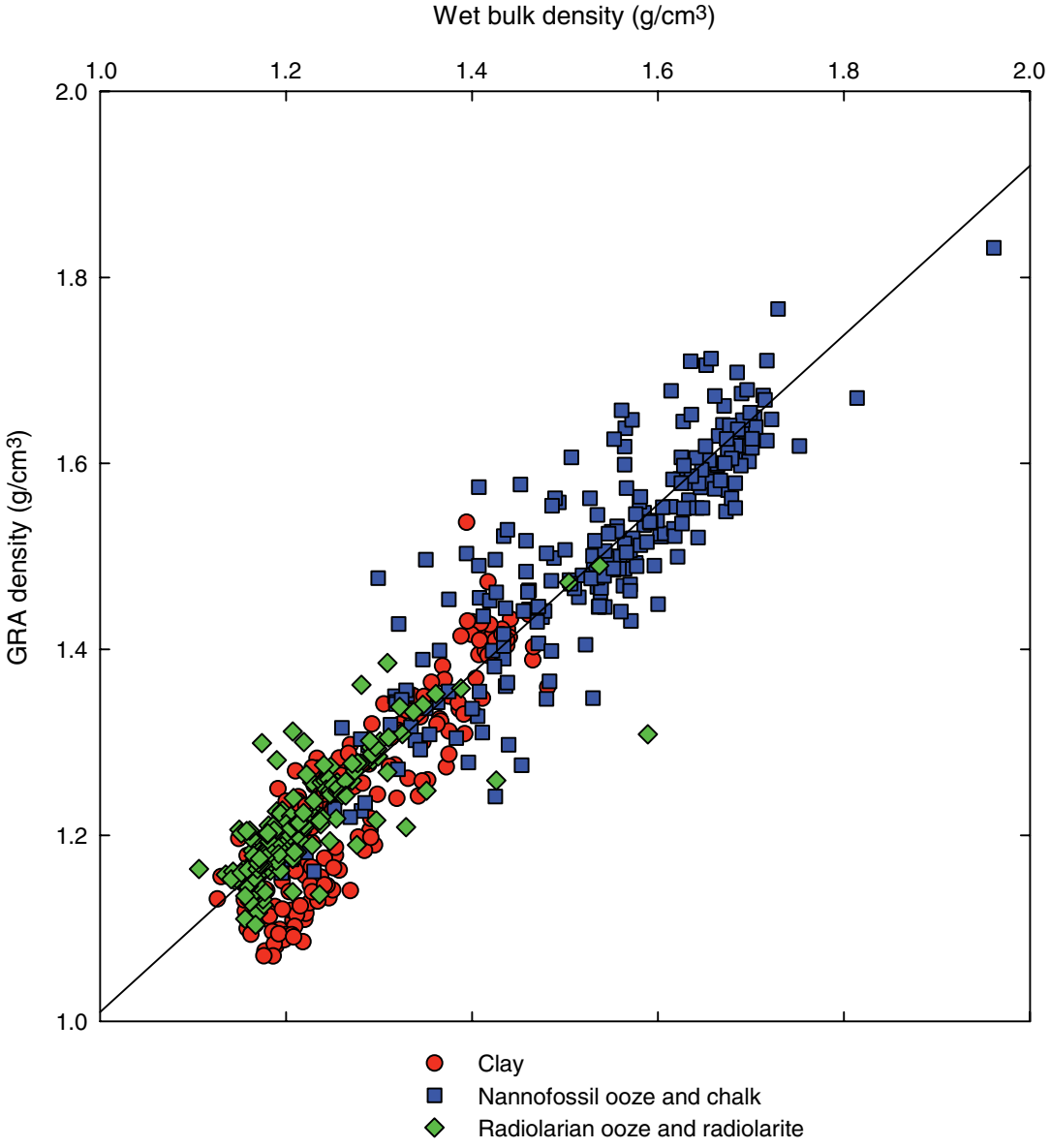

Figure F3. Wet bulk density and porosity for discrete samples. $R^2 = 0.97$. For reference, the variation of wet bulk density with porosity for sediment with interstitial fluid density of 1.024 g/cm³ and varying grain densities (ρ_s) is shown.

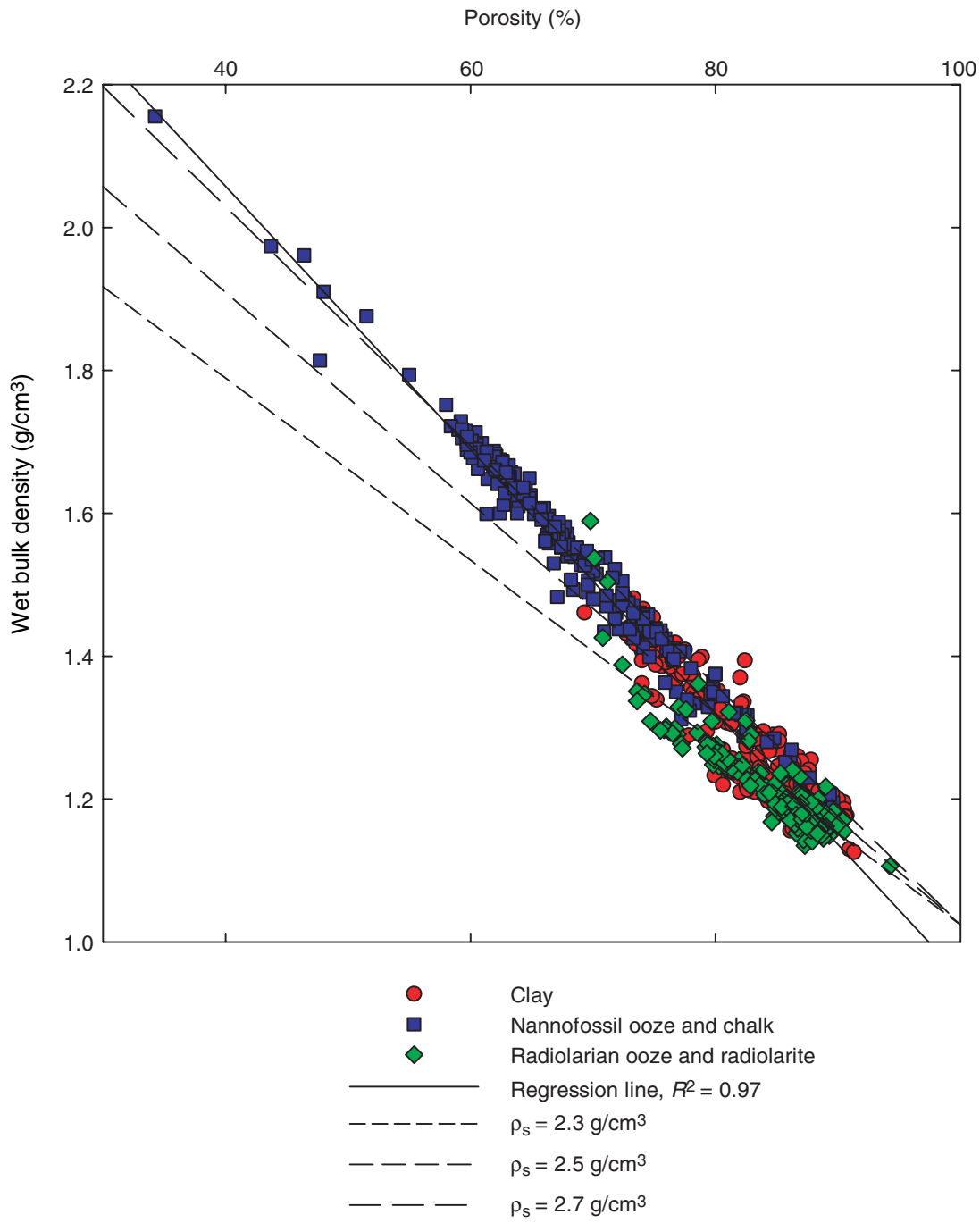

Figure F4. Horizontal *P*-wave velocity as measured by insertion probe and contact probe systems (discrete samples) and MST *P*-wave logger.

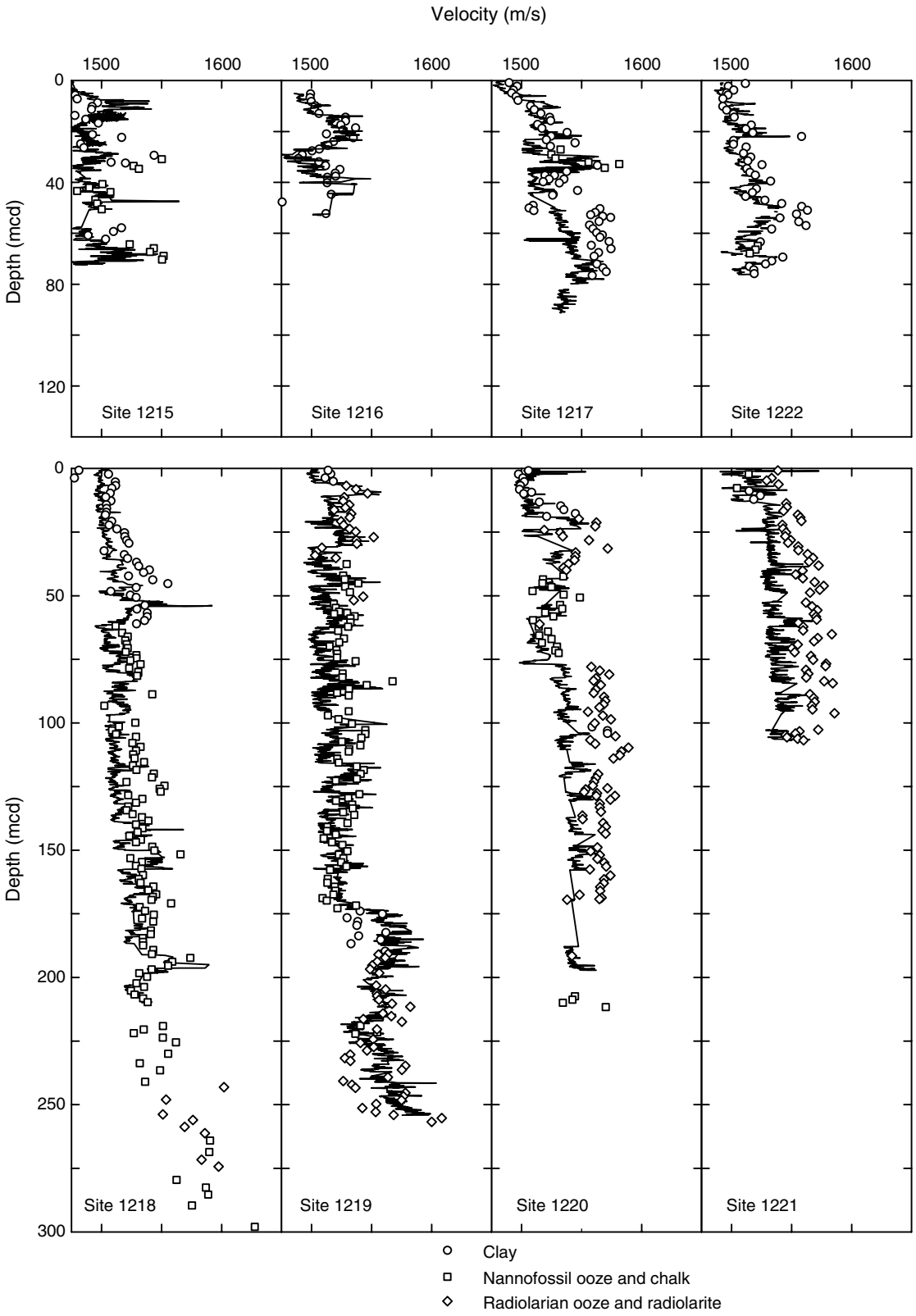

Figure F5. Comparison of the horizontal *P*-wave velocity determined for discrete samples and the *P*-wave logger (PWL) velocity at equivalent depth. $R^2 = 0.59$.

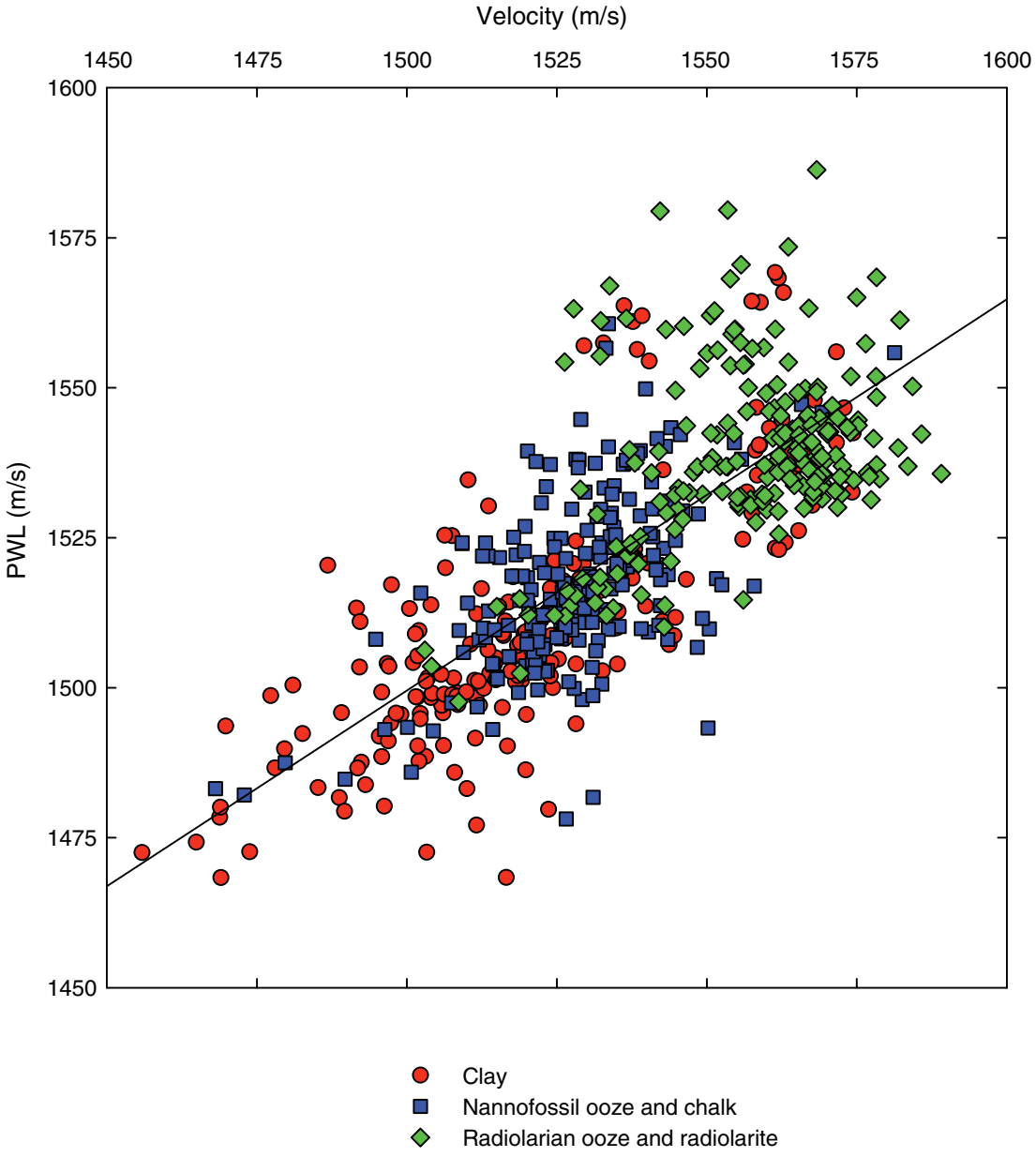

Figure F6. Wet bulk density and velocity for discrete samples.

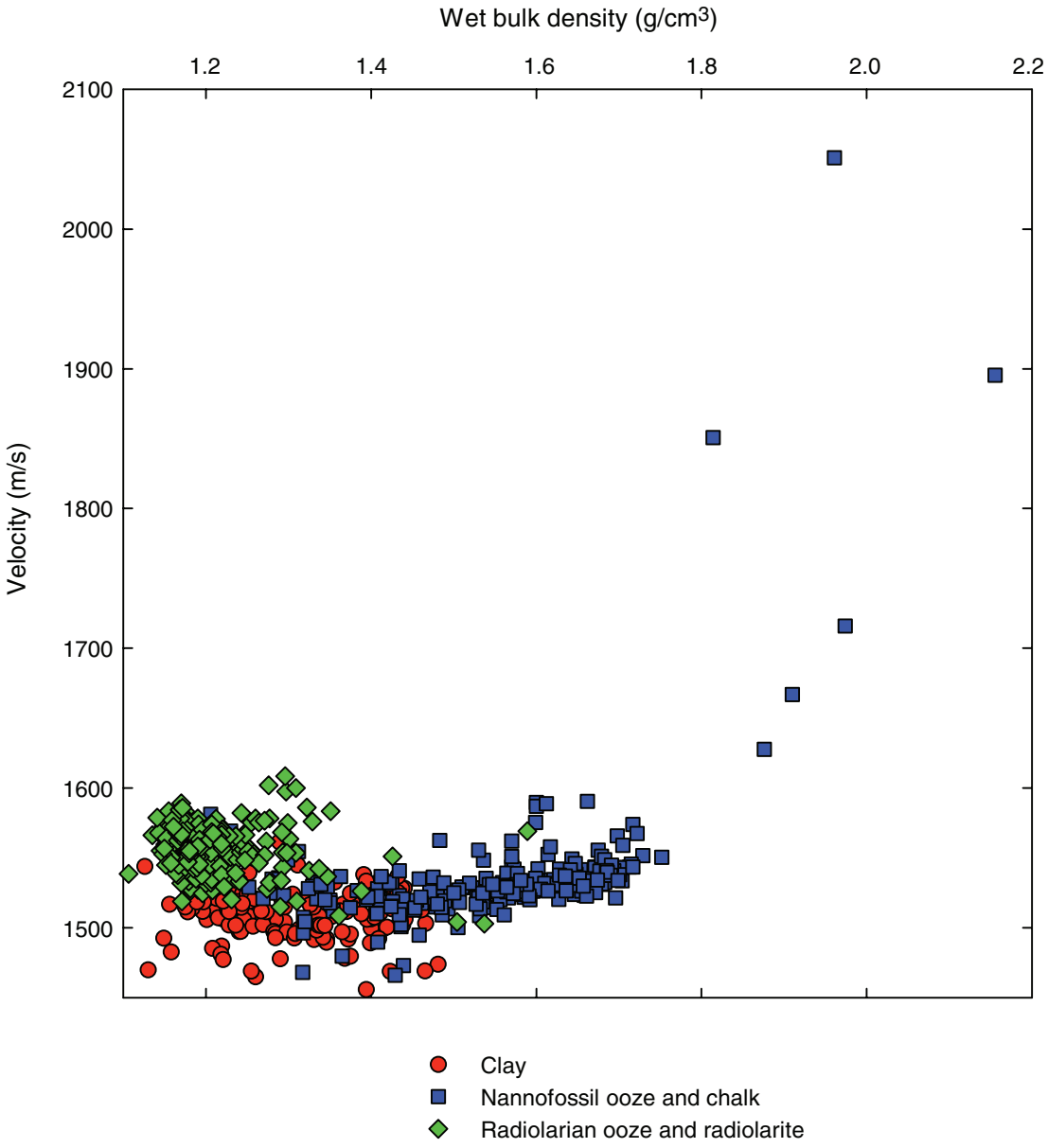

Figure F7. Calcium carbonate content and wet bulk density for discrete samples. $R^2 = 0.73$.

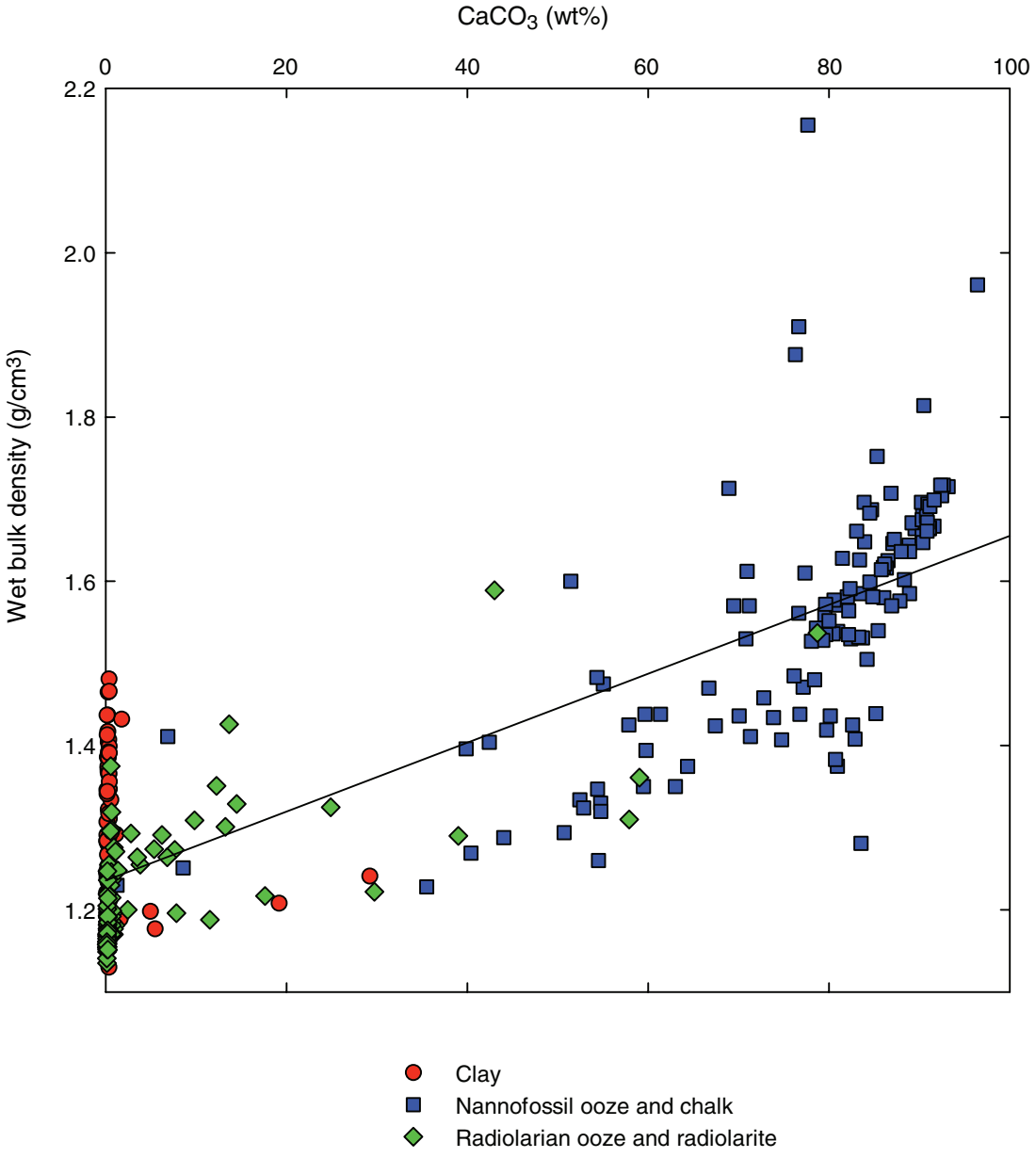

Figure F8. Calcium carbonate content and velocity for discrete samples.

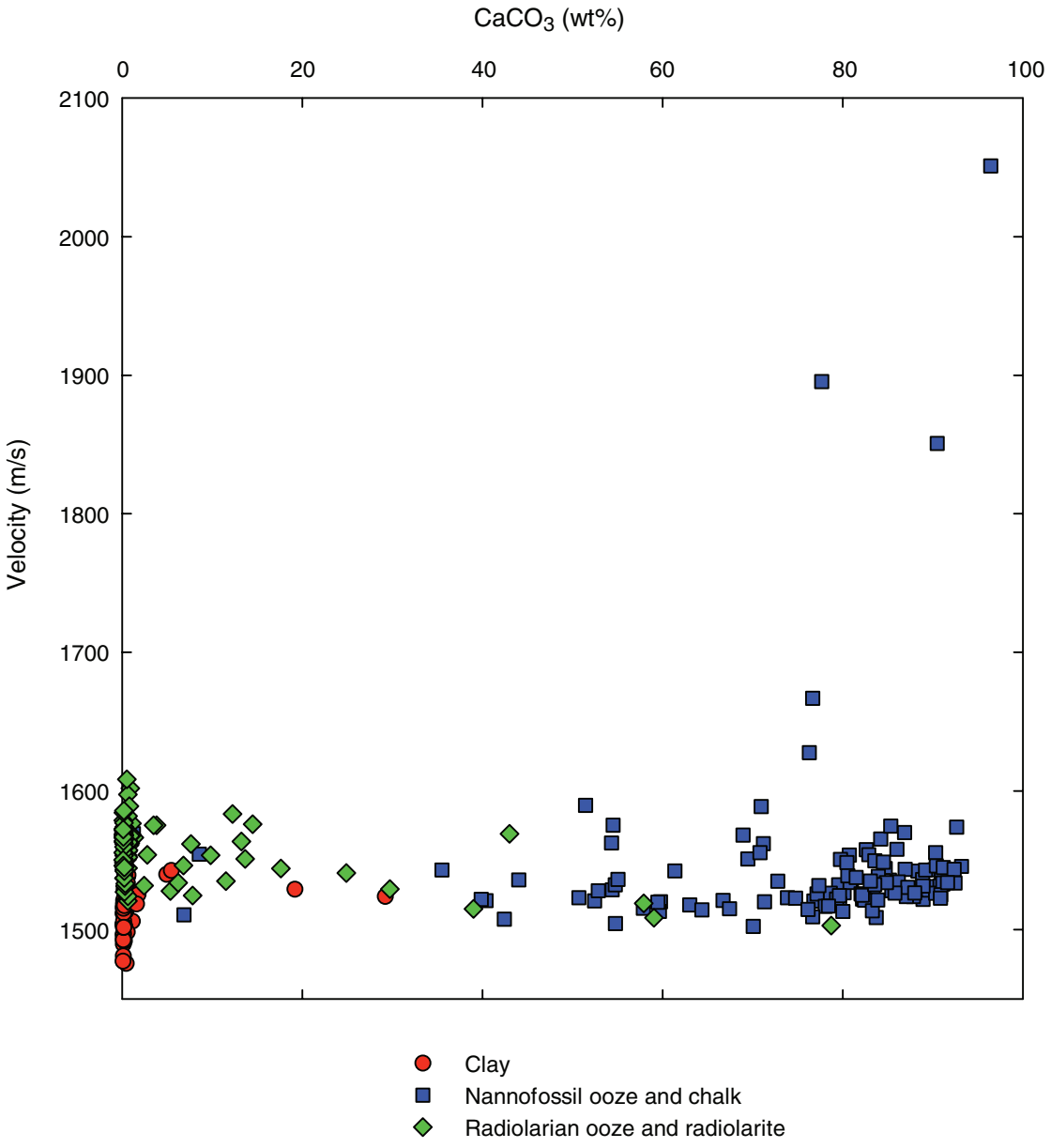

Figure F9. Depth profiles of MST gamma ray attenuation (GRA) and logging Hostile Environment Lithodensity Tool (HLDT) density for Sites 1218 and 1219. GRA depths, originally in mcd, have been shifted to obtain the best match with the logging densities.

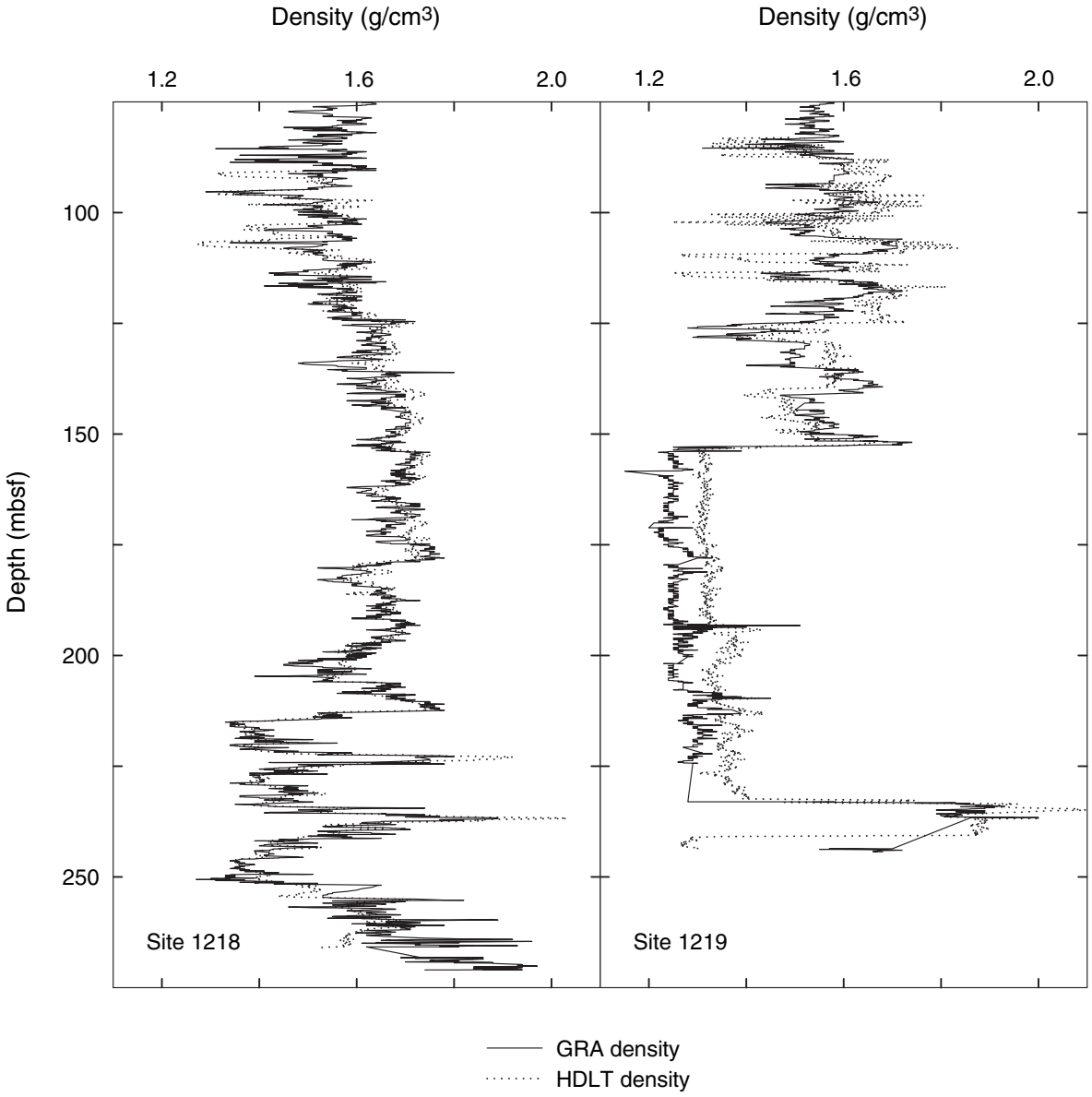

Figure F10. Comparison of MST gamma ray attenuation (GRA) and logging Hostile Environment Lithodensity Tool (HLDT) density at equivalent depths. The line represents the one-to-one relationship between the two densities.

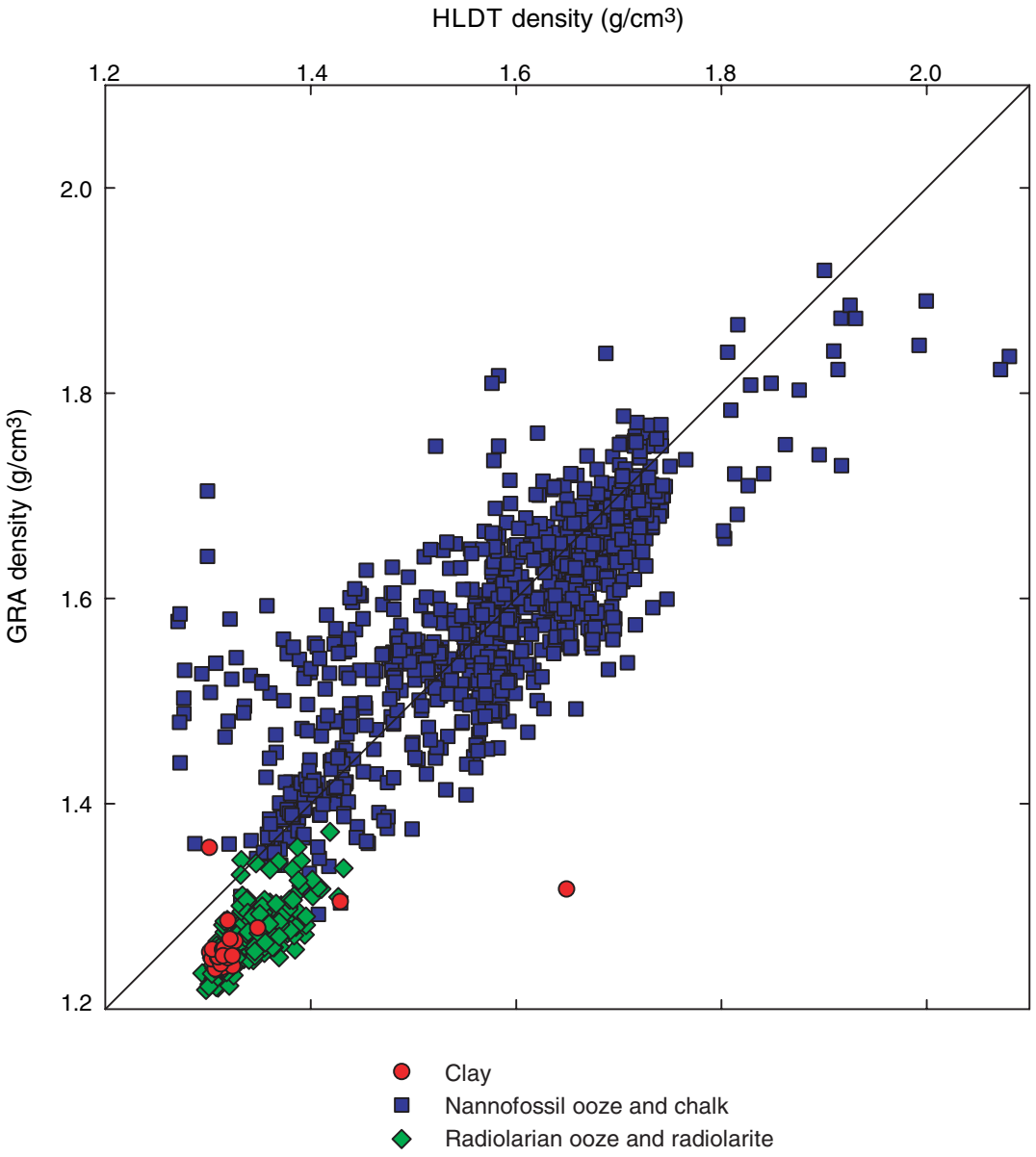

Figure F11. Density difference between the logging density and GRA density (density rebound), averaged over 5-m windows, vs. effective overburden pressure.

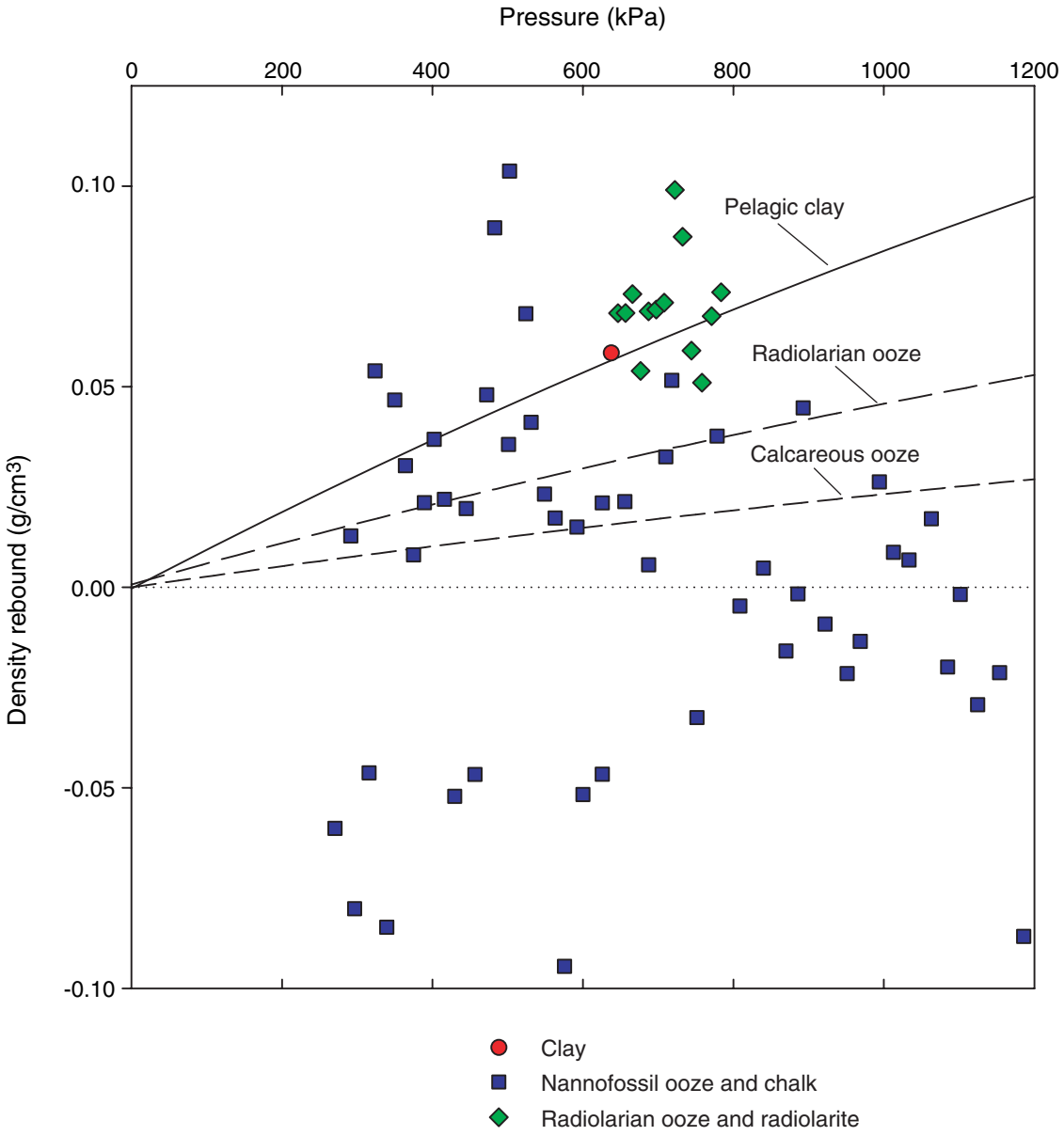

Figure F12. Composite depth profile of rebound-corrected wet bulk density for Leg 199 sites.

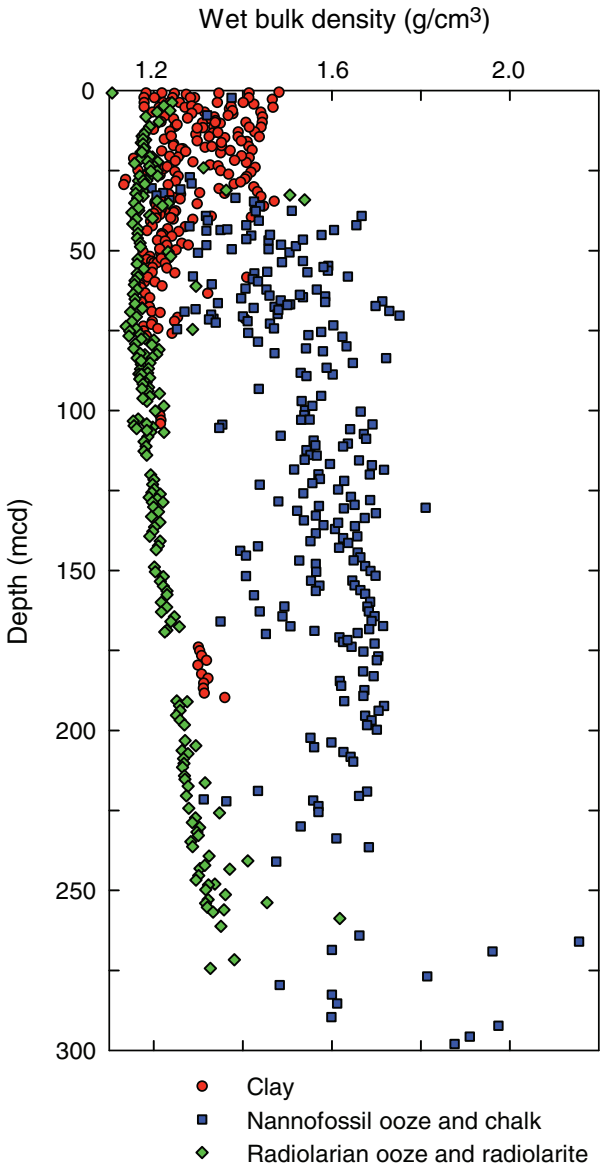

Figure F13. Composite depth profile of corrected velocity for Leg 199 sites.

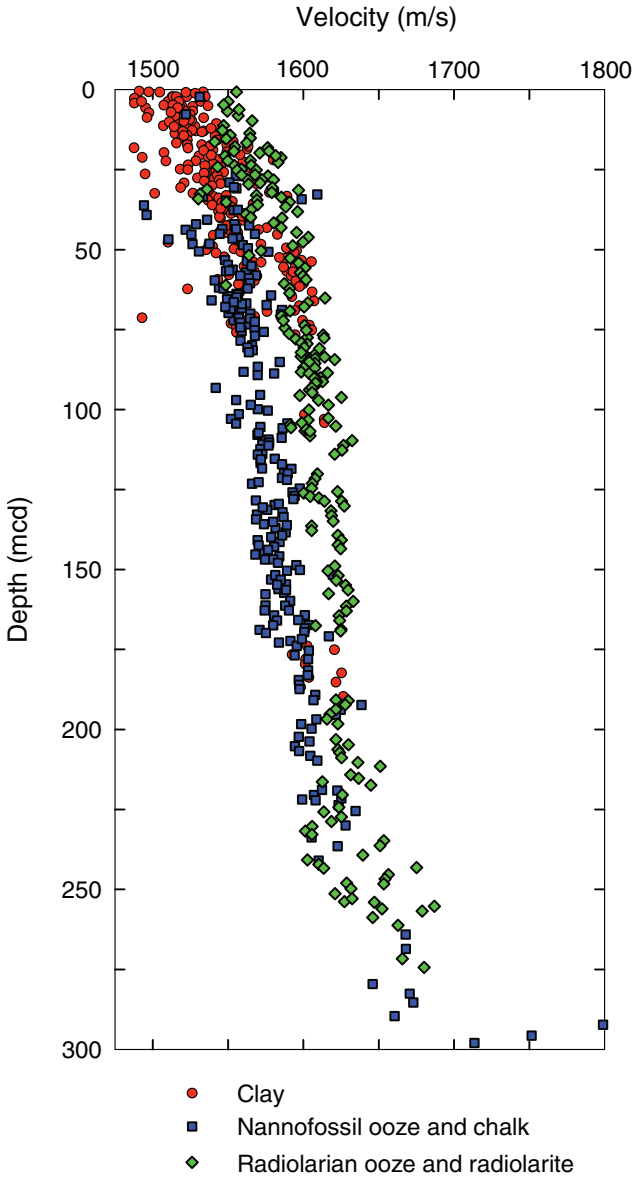

Figure F14. Crossplot of corrected wet bulk density and impedance.

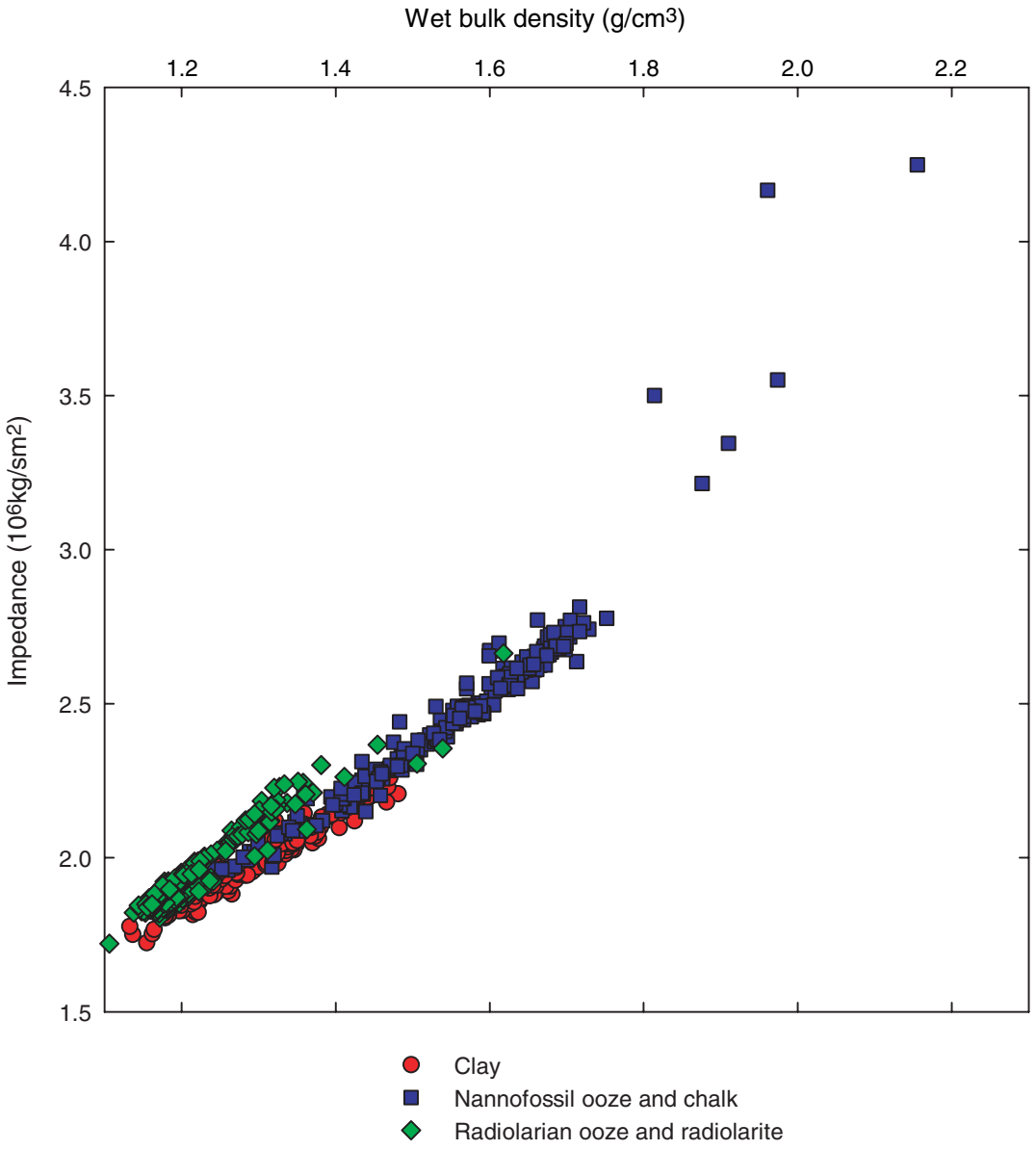

Figure F15. Crossplot of corrected velocity and impedance.

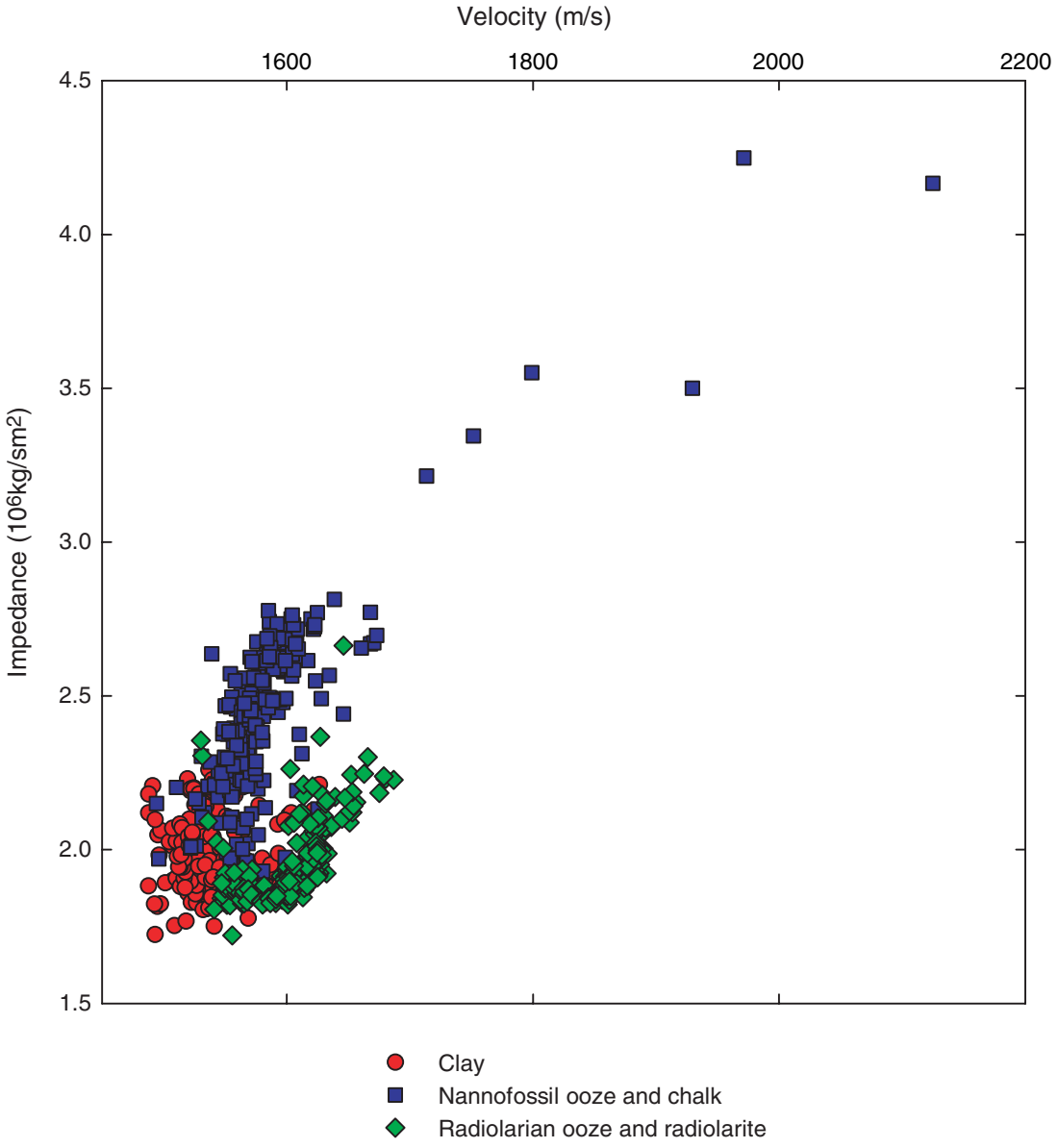

Table T1. Stepwise multiple regression of wet bulk density with LAS data.

Model (independent variables)	Adjusted R^2
Calcite	0.73
Calcite, opal	0.78
Calcite, opal, depth	0.86
Calcite, opal, depth, illite	0.87

Note: $N = 680$.

Table T2. Stepwise multiple regression of velocity with LAS data.

Model (independent variables)	Adjusted R^2
Depth	0.19
Depth, opal	0.25
Depth, opal, illite	0.25

Note: $N = 657$.

Table T3. Stepwise multiple regression of wet bulk density with sediment bulk geochemistry data.

Model (independent variables)	Adjusted R^2
Ca	0.63
Ca, Ti	0.68
Ca, Ti, depth	0.81
Ca, Ti, depth, Sr	0.82
Ca, Ti, depth, Sr, Ba	0.83
Ca, Ti, depth, Sr, Ba, Si	0.84
Ca, Ti, depth, Sr, Ba, Si, Al	0.87
Ca, Ti, depth, Sr, Ba, Si, Al, Mg	0.87

Note: $N = 432$.

Table T4. Stepwise multiple regression of velocity with sediment bulk geochemistry data.

Model (independent variables)	Adjusted R^2
Depth	0.22
Depth, Sr	0.3
Depth, Sr, Ca	0.41
Depth, Sr, Ca, Ti	0.43
Depth, Sr, Ca, Ti, Ba	0.43

Note: $N = 436$.